EVE Doppler Signatures in Major Flares

Hugh Hudson (Berkeley and Glasgow), Phil Chamberlin (NASA/GSFC),
Alec MacKinnon (Glasgow) and Tom Woods (LASP)

Background: This poster describes SDO/EVE spectroscopy of the Sun as a star in the EUV (see Hudson et al., 2011 Woods et al. 2012, and Chamberlin, 2016 for details). In this presentation we discuss the behavior of the transition-region lines, aiming at an eventual "calibration" via AIA imagery of the phenomena we see in this novel way. Future stellar observations may thus recognize common paradigms.

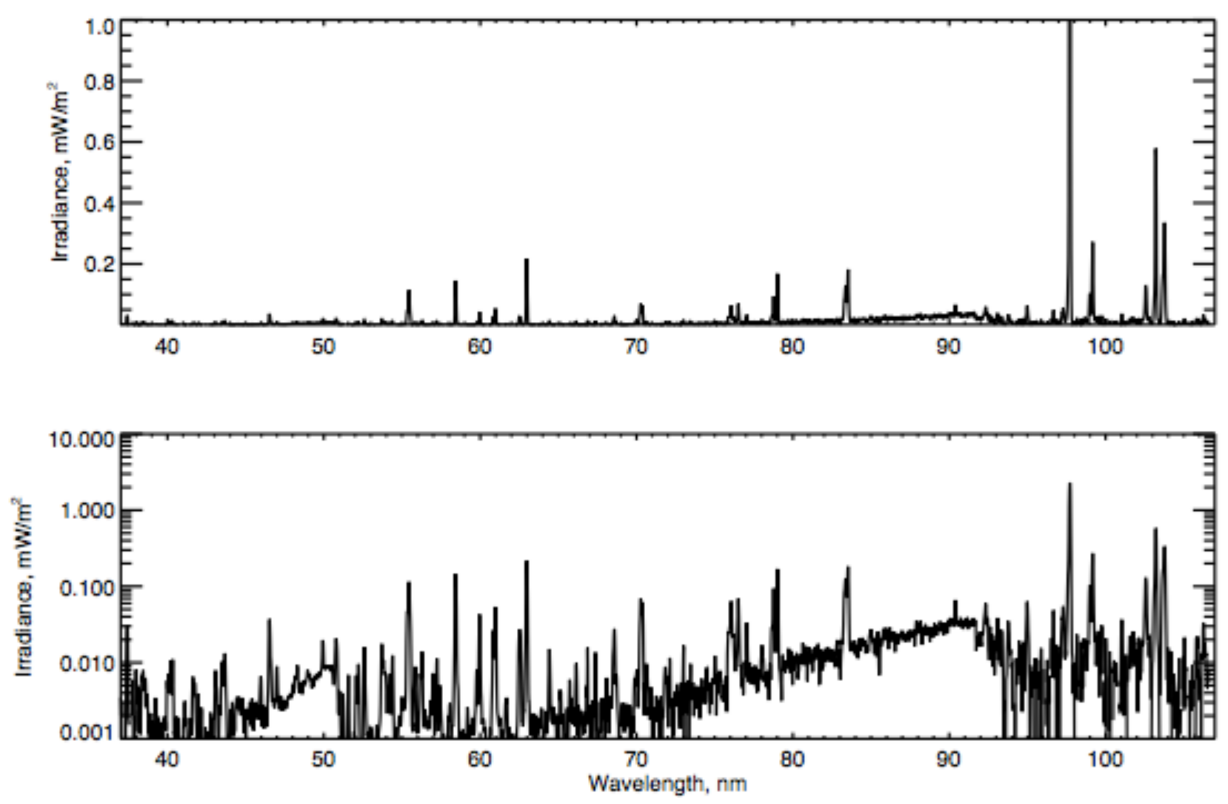

Figure 1. Representative flare excess spectrum from EVE/MEGS-B, in linear and log versions, showing the wealth of lines available. This represents one 10-s data integration differenced against a 200-s integration prior to the SOL2011-07-30 (M9.7), taken at flare maximum time.

Table 1. Major flares for which MEGS-B spectroscopy is available. The rise time is from GOES, the log derivative time.

Flare	GOES	Location	Ne IV $\mu W/m^2$	τ_{rise} s
SOL2011-02-15T01	X2.2	S20W10	9.35± 0.15	378
SOL2011-02-16T14	M1.6	S20W32	8.72± 0.13	152
SOL2011-03-07T19	M3.7	N30W48	9.41± 0.15	1314
SOL2011-07-30T02	M9.3	N15E35	8.78± 0.13	114
SOL2011-08-04T03	M9.3	N19W36	8.99± 0.12	295
SOL2012-03-07T00	X5.4	N18E31	9.27± 0.12	628
SOL2012-03-14T15	M2.8	N14E05	9.17± 0.11	290
SOL2012-05-10T20	M1.7	N12E12	9.11± 0.14	373
SOL2012-06-30T18	M1.6	N14E18	9.25± 0.13	119
SOL2012-07-01T18	M2.8	N14E04	9.31± 0.13	191
SOL2012-07-02T20	M3.8	S17W01	9.82± 0.12	451
SOL2014-01-01T19	M9.9	S16W45	9.85± 0.14	286
SOL2014-01-07T18	X1.2	S12W08	9.46± 0.12	890

Table 2. Useful lines in the MEGS-B flare spectra. We exclude the He lines here.

Element	Ion	log(T) CHIANTI	EVE bin	Wavelength Å
Fe	XVI	6.8	1653	360.7590
Ne	VII	5.7	2176	465.2200
Si	XII	6.9	2346	499.4066
He	I	4.5	2428	515.6180
Si	XII	6.0	2453	520.6661
He	I	4.5	2462	522.2140
O	III	5.0	2479	525.7940
He	I	4.5	2535	537.0310
Ne	IV	5.2	2569	543.8860
Al	XI	6.9	2600	550.0318
O	IV	5.2	2622	554.1585[a]
Ne	VI	5.6	2664	562.7030
Ne	V	5.4	2711	572.3360
He	I	4.5	2771	584.3350
O	III	4.9	2848	599.5900
Mg	X	6.8	2974	624.9426
O	V	5.3	2999	629.7320
N	III	4.9	3279	685.8170
O	III	4.9	4026	835.2890
C	III	4.8	4736	977.0200
N	III	4.8	4808	991.5770
O	VI	5.4	5010	1031.9138
O	VI	5.4	5038	1037.6154

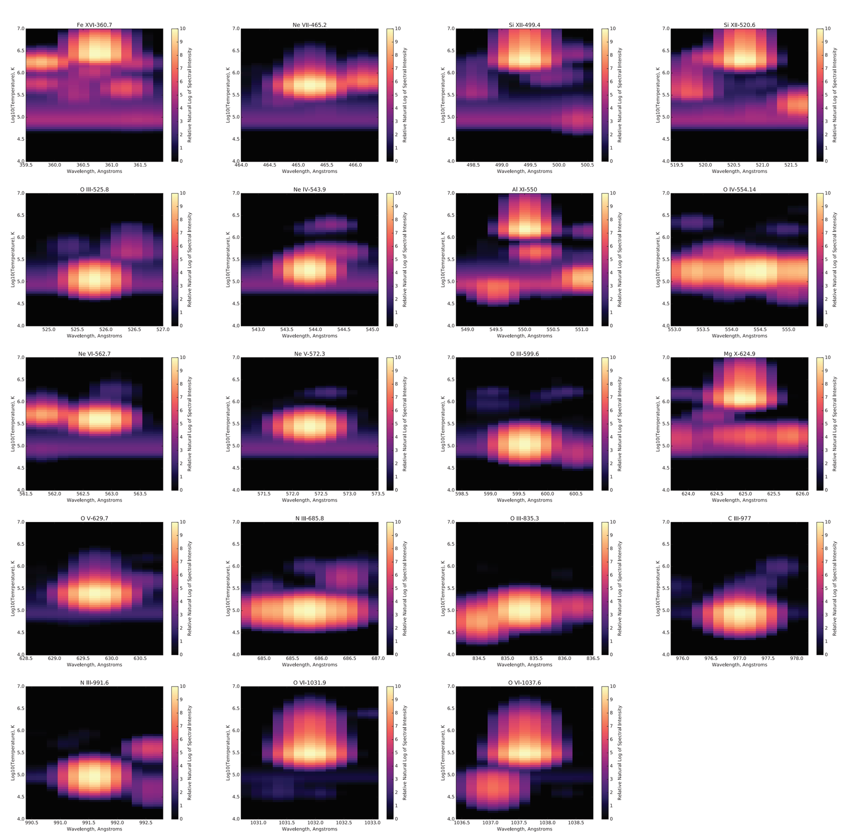

Figure 2. "Blend maps" from CHIANTI (Dere et al. 1997; Landi et al. 2013). Each panel shows one of the lines in Table 2, omitting He, across the range of a standard Gaussian fit (0.22 nm) and the temperature range 10^4-10^7 K. The color scale covers five decades of CHIANTI extended-flare DEM intensity for the temperature range 10^4-10^7 K.

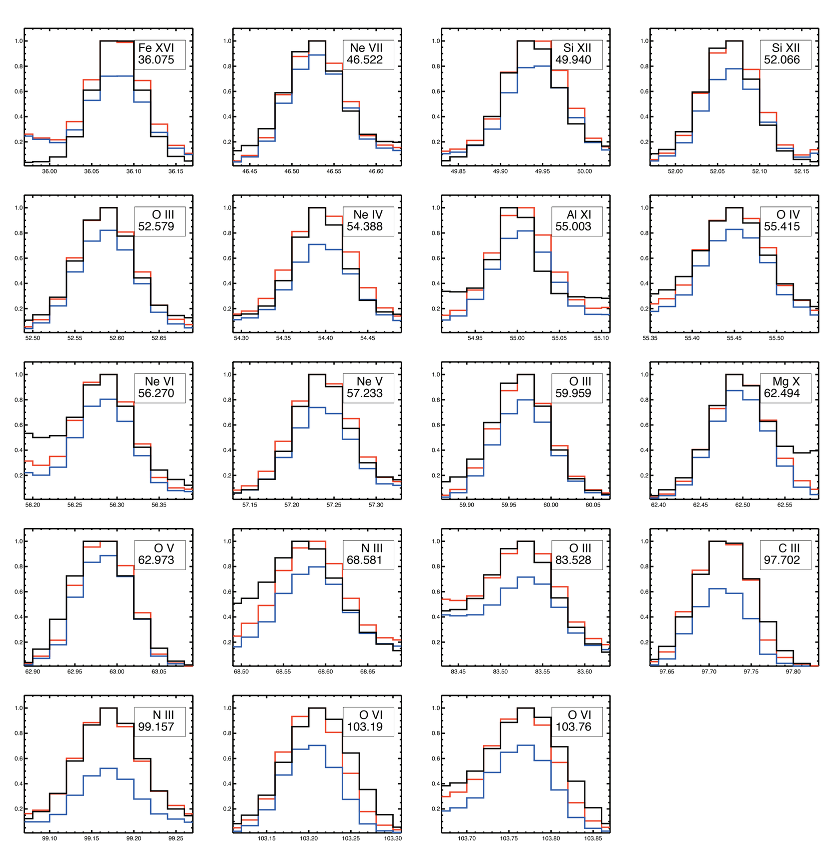

Figure 3. Standard Gaussian fits for the chosen lines as seen in SOL2012-07-30, using a standard six-parameter model to extract one line and a quadratic background term. The plots are normalized to the flare excess peak (black), with blue and red showing the preflare and peak flare spectra, respectively.

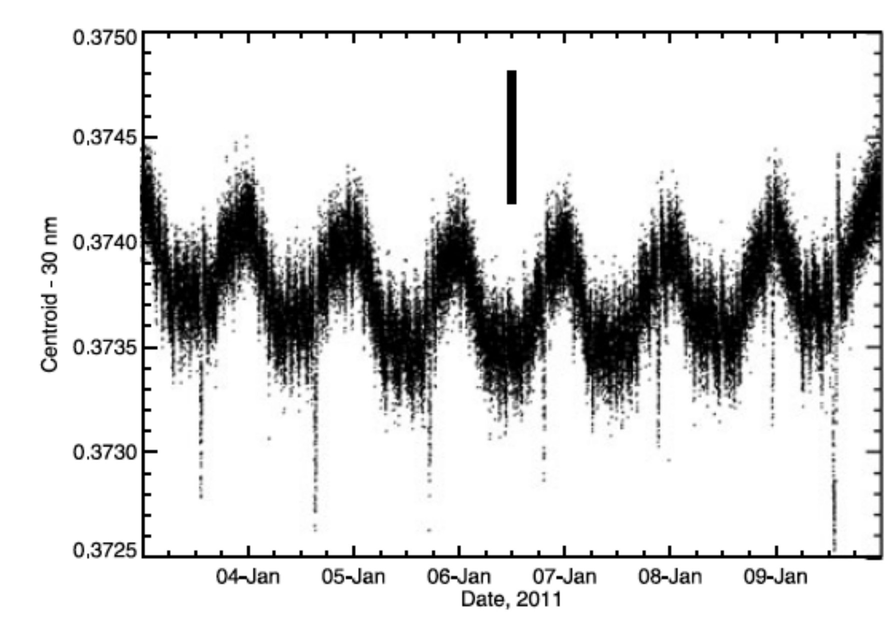

Figure 3. Doppler signature of SDO orbital motion as detected in He II 30.4 nm (Hudson et al. 2011). The vertical bar is 3 km/s.

References

Chamberlin, P.C., Solar Phys. **291**, 1665 (2016) – EVE/MEGS
Dere, K. et al. 1997, A&A Supp., **125**, 149 (1997) – CHIANTI
Hudson, H. et al., Solar Phys. **273**, 69 (2011) – EVE spectral shifts
Landi, E. et al., ApJ, **763**, 86 (2013) – CHIANTI
Milligan, R.O. and Dennis, B.R., ApJ, **699**, 968 (2007) – Flare Doppler patterns
Woods, T. et al., Solar Phys. **275**, 115 (2012) – EVE

MEGS-B vs. MEGS-A

Our previous published work on EVE Doppler measurements (Hudson et al. 2011) used MEGS-A. This instrument observes high-excitation lines well, but has the technical problem that these lines do not form outside flare times, and so rest reference spectra are not easily found. This is important because of the wavelength/spectrum coupling (an optical design property; see Woods et al., 2012, and Chamberlin, 2016).

For MEGS-B these problems are unimportant. We can use pre-flare emission safely as a rest reference. Accordingly, the results presented here focus on transition-region lines with peak formation temperatures below 1 MK; such lines are always available in the spectra. In this analysis we use the line set in Table 2 here, omitting the He lines and two others upon close inspection. See Figures 2 and 3 for "blend maps" and line profiles in one flare event.

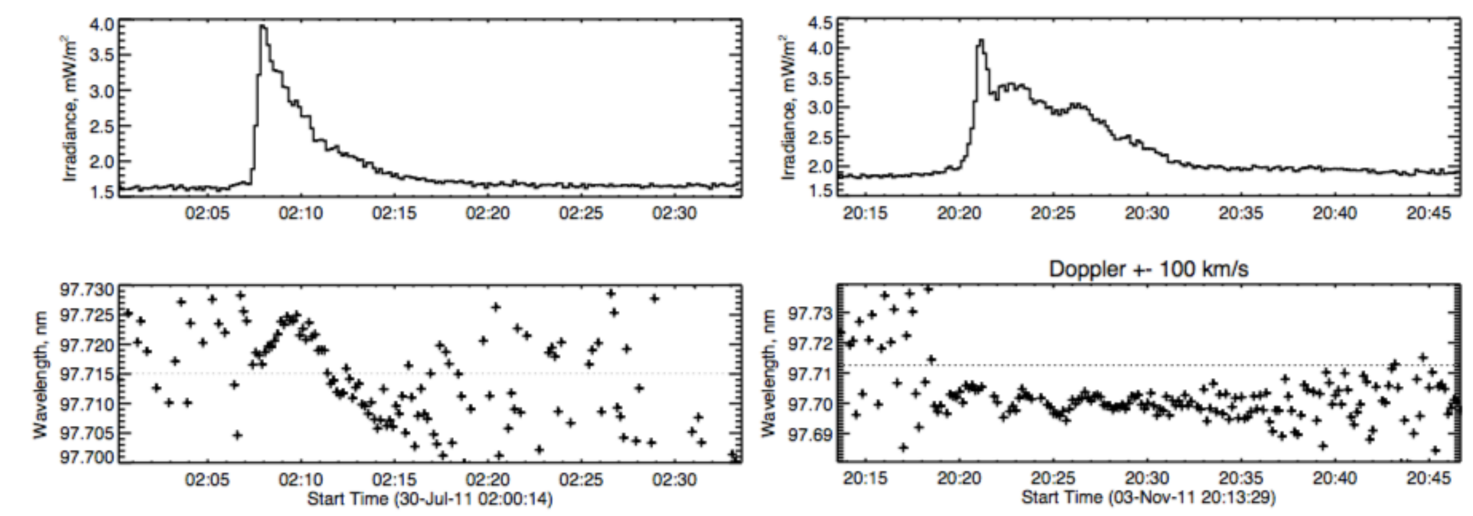

Figure 4. Time series of Doppler measurements for two flares in C III 97.7 nm. SOL2011-07-30 (left) shows a swing from red, in the impulsive phase, to blue in the gradual phase. SOL2011-11003 shows a persistent blueshift. At this wavelength 10 pm = 31 km/s.

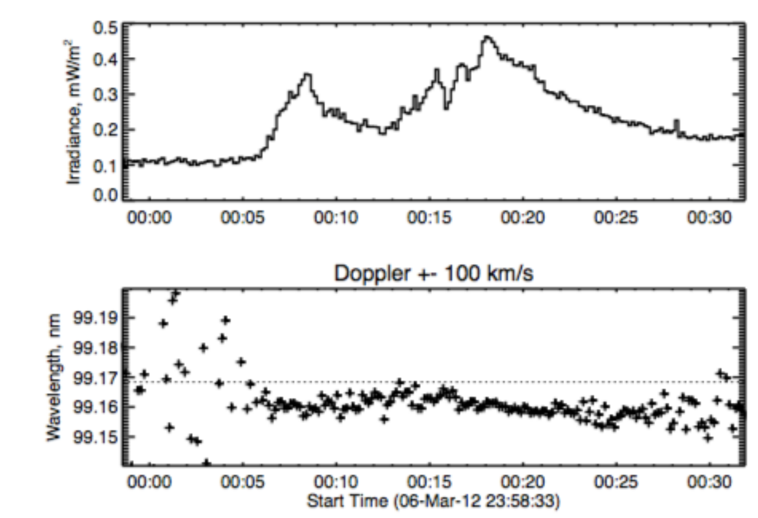

Figure 5. Another flare with blueshifts in transition-region lines, in this case N III 99.1 nm

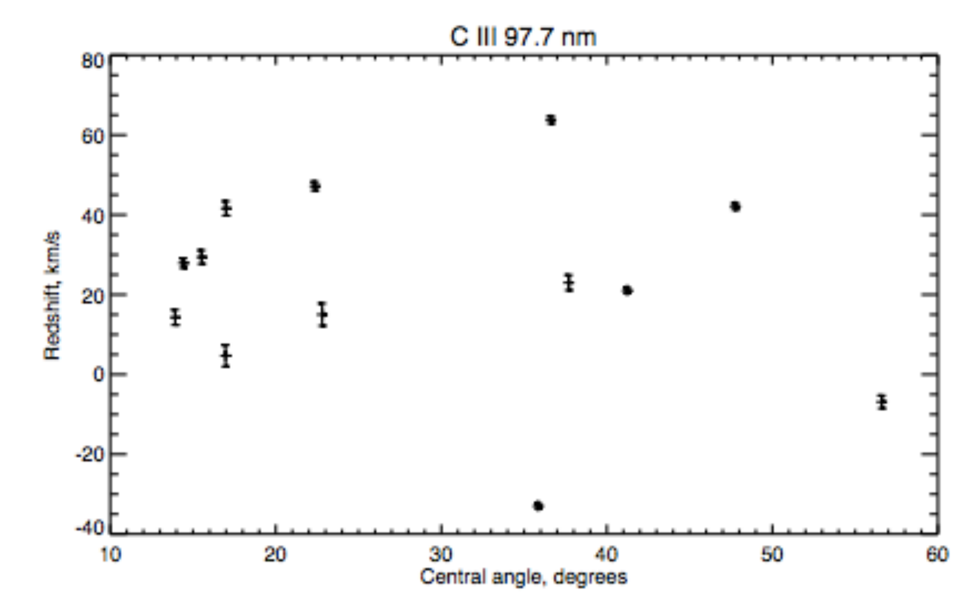

Figure 6. Redshifts at GOES maximum for all flares in the C III line, plotted here against central angle. Typical uncertainties are of order 1 km/s here. As one can see from the time-series plots (Figs. 4 and 5) the variation of the mean Doppler flows is well measured by EVE. Various other correlations have been sought and not found; the working hypothesis is that there is no systematic pattern and that the uncorrelated variance comes from the details of the flare structures. In the next phase of analysis, we intend to carry out a detailed survey of AIA imagery in an effort to identify this structural dependence.

Conclusions

EVE/MEGS-B sees transition-line Doppler shifts well. In this survey we are finding mean velocities of +-10s of km/s:

a) C III, the strongest line, can exhibit either blue or red shifts, with precision of order 1 km/s.
b) N III tracks C III well, suggesting that EVE can measure mean temperature *gradients.*
c) There is a large uncorrelated flare-to-flare variance that we hope to identify, via AIA, with flare structural detail.
d) The pattern of Doppler shift vs temperature is not as simple as one sees in the classic work of Milligan & Dennis (2009).
e) The body of work enabled by EVE should really help to disentangle paradigms for related stellar observations.